SIMULATION OF DIELECTRIC WAKEFIELD ACCELERATION IN PLANAR STRUCTURES AT SwissFEL

E. Ericson*[,1,2], P. Craievich[1], R. Ischebeck[1], F. Marcellini[1], M. Seidel[1,2]
[1]Paul Scherrer Institute, PSI, Villigen, Switzerland
[2]Ecole Polytechnique Federale de Lausanne, EPFL, Lausanne, Switzerland

Abstract

SwissFEL uses two 1 m-long planar dielectric wakefield structures to manipulate the beam's energy chirp in its hard X-ray beamline, Aramis. Simulations show wakefields generated in the structures that can be used to accelerate witness beams. Many wakefield structures use a high-charge, ~ ps-long drive beam to excite strong accelerating wakes. Here we introduce SwissFEL's dielectric wakefield structures and simulate the wakefields produced inside the structures by ~ fs beams. The longitudinal wake potential dependence on bunch length, structure gap, dielectric thickness and dielectric permittivity is investigated. We find the thickness and permittivity of the structures' dielectric coating determine the location of the first accelerating peak of the wake potential. We compare the longitudinal wake potentials generated in the dielectric structures with those in SwissFEL's planar corrugated metallic structures. Finally, we consider the quadrupole wakefields excited in the structures.

INTRODUCTION

Wakefields structures can manipulate a charged particle beam's phase space. Structures have been designed to generate wakefields to accelerate, streak, dechirp, or energy-modulate particle beams [1–4]. SwissFEL currently has 12 planar wakefield structures installed. The 10 planar metallic corrugated structures and their uses have been previously described [3–6]. Two identically-designed planar dielectric wakefield structures are installed at the end of SwissFEL's 6 GeV linear accelerator (LINAC) [7]. Each structure is made of two parallel girders with aluminium plates coated with alumina dielectric. The separation between a structures girders is adjustable and the two dielectric structures are installed orthogonally relative to each other.

A diagram of one of the structures is shown in Fig. 1. The corresponding parameters are listed in Table 1.

Table 1: Parameters of Each of SwissFEL's Planar Dielectric Wakefield Structures

Parameter	Value
length, L	1000 mm
width, $2w$	42 mm
dielectric thickness, d	0.4 mm
gap, $2a$	0.5–4 mm
dielectric relative permittivity, ϵ_r	10

* evan.ericson@psi.ch

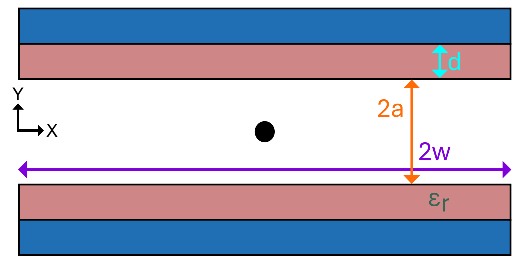

Figure 1: Transverse cross-section of a SwissFEL planar dielectric wakefield structure. The dielectric layer is shown in pink. The beam, shown in black and represented on-axis, generates wakefields as it travels between the dielectric layers. The diagram is not to scale.

SIMULATIONS OF SwissFEL'S PLANAR DIELECTRIC WAKEFIELD STRUCTURES

Figure 2 shows longitudinal wake potentials generated in the structure by various ~ fs bunch lengths. Typically the short-range wakefields are used to reduce the energy of the tail of the beam to reduce the beam's energy chirp. Behind the beam, the wake potentials feature many accelerating peaks typical of a multimode wakefield structure. A bunch train travelling through a multimode structure has been used to resonantly load the wakefields which is believed to drive large accelerating wakefields [8, 9]. The first and largest accelerating peak of the wakes in the SwissFEL structures is located near $t = 8$ ps. The location of the accelerating peak does not change significantly with structure gap. We expect the simulation would predict further damping of the wake if the simulation included complex permittivity [10]. The ECHO2D simulations [11] assumed a pencil beam travelled on-axis and the dielectric surface was flat. The high-frequency oscillations in the wake potentials are numerical artifacts that vanish when the mesh is refined [12].

For a fixed structure gap, the accelerating gradient can be increased by either increasing the drive beam charge, decreasing the drive beam length, or both. The amplitude of the accelerating peaks in Fig. 2 suggests as the bunch length is reduced, the wake potential's maximum accelerating gradient reaches a plateau close to 0.2 MV/pC/m. The bunch length-independent wake potential corresponds to the structure's single-particle wake function. For SwissFEL's 200 pC beam and combined 2 m of structure, the peak unloaded accelerating wake corresponds to a ~40 MV/m accelerating gradient. At larger structure gaps, the wake potential saturates at lower amplitude and for a longer bunch. A structure with an adjustable gap may be useful for schemes to iteratively center the structure about the beam.

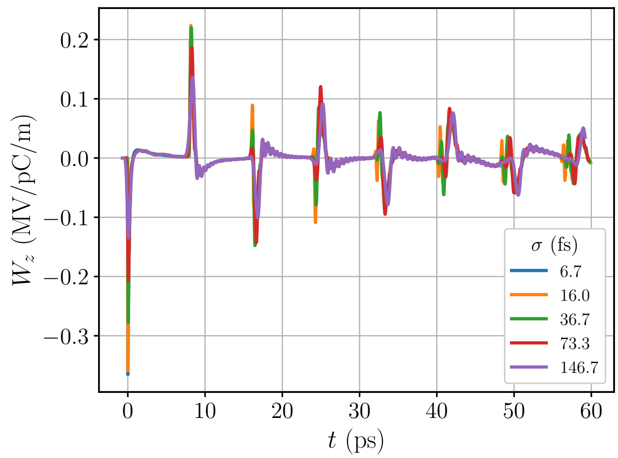

Figure 2: Longitudinal wake potential of the SwissFEL planar dielectric structures generated using bunch lengths similar to those achievable in SwissFEL. The simulated structure had a gap of $2a = 0.5$ mm.

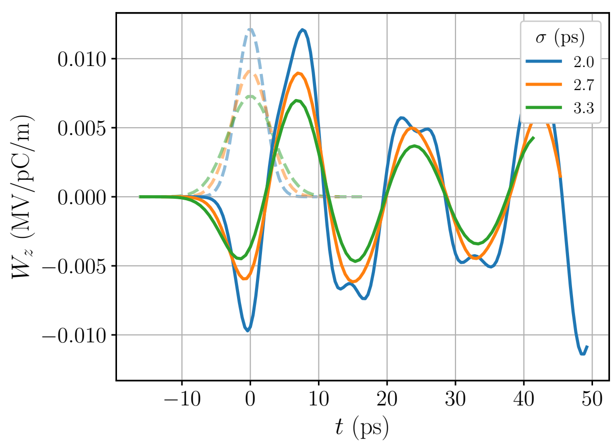

Figure 3: Longitudinal wake potential of the SwissFEL planar dielectric structures generated using relatively long beams (dashed lines). The simulated structure had a gap of $2a = 0.5$ mm.

When the drive beam length is increased, a single mode can be excited in the structure resulting in a sinusoidal longitudinal wake potential, with smaller amplitude than the short beam case. Figure 3 shows, when $2a = 0.5$ mm, the wakefield becomes sinusoidal when a 3 ps beam passes through the structure. In the SwissFEL injector, the beam is σ = 3 ps, suitable to drive a sinusoidal wake potential [13].

PLANAR DIELECTRIC STRUCTURE PARAMETER SCAN

SwissFEL simultaneously serves two beamlines using two 200 pC bunches nominally separated by 28 ns. Because it is difficult to find a machine configuration to produce a drive-witness pair separated by 8 ps to verify the wakefields predicted by the simulation, we investigated the wakes in different structures. Figure 4 shows the thickness of the alumina coating and its permittivity determine the location and amplitude of the first accelerating peak. For this reason, dielectric materials with tunable permittivity have previously been studied [14,15]. Varying the dielectric permittivity also affects the amplitude and slope of the short-range wakes. The short-range wakes were not sensitive to different dielectric thickness in the range we scanned. The accelerating peak maximum varies with dielectric thickness as well. Dielectric structures with increased thickness and permittivity would have a first accelerating peak closer to the current bunch spacing and a decreased accelerating amplitude.

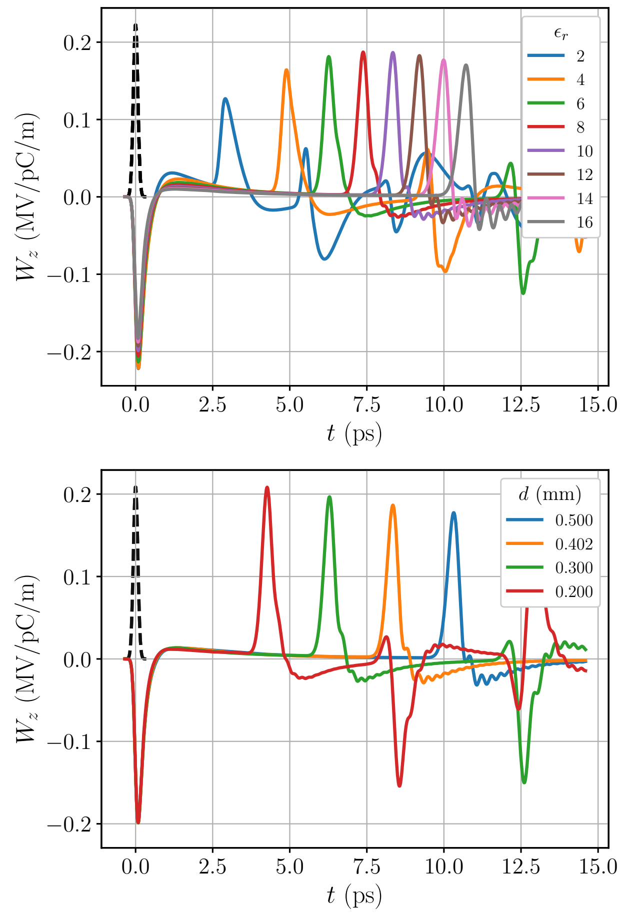

Figure 4: Dielectric permittivity scan with $d = 0.4$ mm (top) and dielectric thickness parameter scan with $\epsilon = 10$(bottom) with a gap of $2a = 0.5$ mm generated by a $\sigma = 74$ fs beam (black dashed lines).

For SwissFEL's ~fs beams, a sinusoidal wake potential can be obtained by using structures with thin coatings. The wake potential generated by a $\sigma = 74$ fs beam becomes sinusoidal for coating thicknesses less than 10 µm. The sinusoidal wake potential damps faster than non-sinusoidal wake potentials generated in the structure.

COMPARISON WITH SwissFEL'S CORRUGATED STRUCTURES

SwissFEL's corrugated structures have been used to manipulate the injector beam's longitudinal phase space [6]. We evaluated the long-range longitudinal wakefields in three different corrugated structures driven by a short beam.

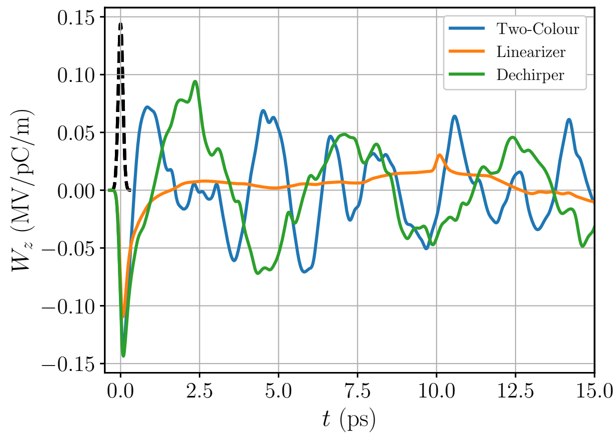

Figure 5: Longitudinal wake potential of SwissFEL's planar corrugated structures with a gap of $2a = 0.5$ mm generated by a $\sigma = 74$ fs drive beam (black dashed line).

Figure 5 shows the planar corrugated metallic structures do not feature distinct accelerating peaks over the same time scale where accelerating peaks were predicted in the dielectric structure wakes. The wakes have accelerating portions with a lower amplitude than the dielectric structures. The wake produced by the dechirper geometry has qualities of a single mode wake modulated by a high frequency mode. For the same beam $\sigma = 74$ fs and structure gaps, $2a = 0.5$ mm, SwissFEL's corrugated structures produce lower amplitude short-range wakepotentials than SwissFEL's dielectric structures.

QUADRUPOLE WAKEFIELDS

Because planar dielectric structures do not have rotational symmetry, quadrupole wakefields are excited even when a beam travels through SwissFel's planar dielectric structures device on-axis. Quadrupole wakefields apply time-dependent focusing which can potentially increase the beam size and emittance [16–19]. When a drive-witness pair travel through the structure, the witness beam experiences the superposition of its own quadrupole fields and those excited by the drive beam. Figure 6 shows the net quadrupole wake seen by a witness beam using drive-witness beam parameters similar to those possible at the Argonne Wakefield Accelerator Facility (AWA). The witness beam experiences quadrupolar wakefields of different signs in its head and tail, passing through a zero-crossing in its core.

The effect of the quadrupole wakefields can be mitigated using different techniques. In general, beams with elliptical transverse cross-sections do not excite quadrupole wakefields as strongly as beams with Gaussian transverse distributions. Alternatively, two planar dielectric wakefield structures with alternating orientations can be used to compensate the quadrupole wakefields generated in each structure by generating quadrupole wakes of opposite sign. In this case, where the witness beam's head and tail experience quadrupole wake potentials of different signs, the effect of the wakes could be minimized by tightly focusing the beam's head and tail.

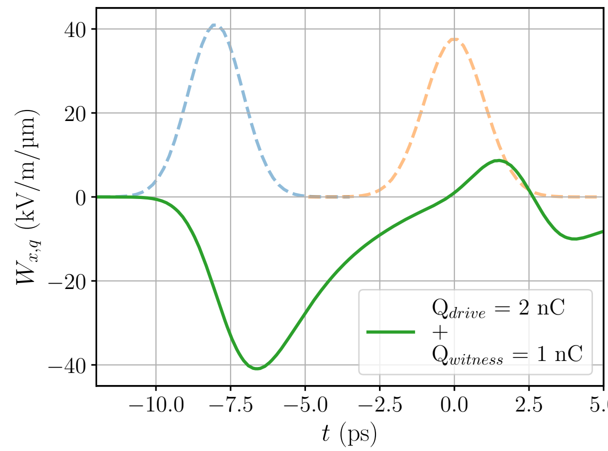

Figure 6: Quadrupole wake potential (green) of SwissFEL's planar dielectric structures with a gap of $2a = 0.5$ mm generated by a $\sigma = 1$ ps, $Q = 2$ nC drive beam (blue) and a $\sigma = 0.9$ ps, $Q = 1$ nC witness beam (orange). In the other plane, $W_{y,q} = -W_{x,q}$.

CONCLUSION

The planar dielectric wakefield structures currently installed at the end of SwissFEL's LINAC can be used for collinear wakefield acceleration. Simulations of the structures' long-range longitudinal wake potentials show an accelerating peak 8 ps behind the drive beam. The dielectric permittivity and dielectric thickness determine the location of the accelerating peak. SwissFEL's planar metallic corrugated wakefield structures produce lower-amplitude accelerating longitudinal wake than the dielectric structures. The quadrupole wakefields generated in the SwissFEL structure using AWA's drive-witness beam results in the witness beam experiencing focusing and defocusing quadrupole wakes.

ACKNOWLEDGEMENTS

The authors would like to Igor Zagorodnov for their help using ECHO2D.

This project has received funding from the European Union's Horizon Europe research and innovation programme under grant agreement No. 101079773.

REFERENCES

[1] G. Andonian *et al.*, "Dielectric wakefield acceleration of a relativistic electron beam in a slab-symmetric dielectric lined waveguide", *Phys. Rev. Lett.*, vol. 108, no. 24, p. 244801, Jun. 2012. doi:10.1103/PhysRevLett.108.244801

[2] P. Dijkstal *et al.*, "Self-synchronized and cost-effective time-resolved measurements at x-ray free-electron lasers with femtosecond resolution", *Phys. Rev. Res.*, vol. 4, no. 1, p. 013017, Mar. 2022. doi:10.1103/PhysRevResearch.4.013017

[3] S. Bettoni *et al.*, "Beam Manipulation Using Self-Induced Fields in the SwissFEL Injector", in *Proc. 9th Int. Part. Accel. Conf. (IPAC'18)*, Apr.–May 2018, pp. 3401–3404. doi:10.18429/JACoW-IPAC2018-THPAK074

[4] S. Bettoni *et al.*, "Beam manipulation using self-induced fields at the SwissFEL injector", in *Proc. 10th Int. Part. Accel. Conf. (IPAC'19)*, May 2019, pp. 266–269. doi:10.18429/JACoW-IPAC2019-MOPGW073

[5] S. Bettoni, E. Prat, and S. Reiche, "Two-color beam generation based on wakefield excitation", *Phys. Rev. Accel. Beams*, vol. 19, no. 5, p. 050702, 2016. doi:10.1103/PhysRevAccelBeams.19.050702

[6] S. Bettoni *et al.*, "Experimental demonstration of two-color x-ray free-electron-laser pulses via wakefield excitation", *Phys. Rev. Accel. Beams*, vol. 24, no. 8, p. 050702, Aug. 2021. doi:10.1103/PhysRevAccelBeams.24.082801

[7] E. Prat *et al.*, "A compact and cost-effective hard X-ray free-electron laser driven by a high-brightness and low-energy electron beam", *Nat. Photonics*, vol. 14, no. 12, pp. 748–754, Dec. 2020. doi:10.1038/s41566-020-00712-8

[8] T.-B. Zhang, J. L. Hirshfield, T. C. Marshall, and B. Hafizi, "Stimulated dielectric wake-field accelerator", *Phys. Rev. E*, vol. 56, pp. 4647–4655, 1997. doi:10.1103/PhysRevE.56.4647

[9] J. G. Power, M. E. Conde, W. Gai, R. Konecny, P. Schoessow, and A. D. Kanareykin, "Measurements of the longitudinal wakefields in a multimode, dielectric wakefield accelerator driven by a train of electron bunches", *Phys. Rev. Spec. Top. Accel. Beams*, vol. 3, p. 101302, 2000. doi:10.1103/PhysRevSTAB.3.101302

[10] A. D. Kanareykin and A. V. Tyukhtin, "Analysis of multimode wakefield generation in accelerating structures with conductive dielectric loading", *Nucl. Instrum. Methods Phys. Res. A*, vol. 558, no. 1, pp. 62–65, Mar. 2006. doi:10.1016/j.nima.2005.11.015

[11] I. Zagorodnov, K. LF. Bane, and G. Stupakov, "Calculation of wakefields in 2D rectangular structures", *Phys. Rev. Spec. Top. Accel. Beams*, vol. 18, no. 10, pp. 1–14, 2015. doi:10.1103/PhysRevSTAB.18.104401

[12] I. Zagorodnov and T. Weiland, "TE/TM field solver for particle beam simulations without numerical Cherenkov radiation", *Phys. Rev. Spec. Top. Accel. Beams*, vol. 8, no. 4, pp. 73–87, 2005. doi:10.1103/PhysRevSTAB.8.042001

[13] G. L. Orlandi, "Absolute and non-invasive determination of the electron bunch length in a free electron laser using a bunch compressor monitor", *Sci. Rep.*, vol. 14, no. 1, p. 6319, Dec. 2024. doi:10.1038/s41598-024-56586-1

[14] A. D. Kanareykin, I. L. Sheinman, and A. M. Al'tmark, "Frequency Control in Wake Field Waveguide Structures", *Tech. Phys. Lett.*, vol. 28, no. 11, pp. 916–918, 2002. doi:10.1134/1.1526882

[15] A. Kanareykin, E. Nenasheva, S. Karmanenko, and V. Yakovlev, "New Low-Loss Ferroelectric Materials for Accelerator Applications", in *Adv. Accel. Concepts 11th Workshop*, pp. 1016–1024, Dec. 2004. doi:10.1063/1.1842656

[16] C. Lu *et al.*, "Time-resolved measurement of quadrupole wakefields in corrugated structures", *Phys. Rev. Accel. Beams*, vol. 19, no. 2, p. 020706, 2016. doi:10.1103/PhysRevAccelBeams.19.020706

[17] F. Fu *et al.*, "Demonstration of nonlinear-energy-spread compensation in relativistic electron bunches with corrugated structures", *Phys. Rev. Lett.*, vol. 114, no. 11, p. 114801, Mar. 2015. doi:10.1103/PhysRevLett.114.114801

[18] Y. C. Chao, W. Qin, Y. Ding, A. A. Lutman, and T. Maxwell, "Control of the Lasing Slice by Transverse Mismatch in an X-Ray Free-Electron Laser", *Phys. Rev. Lett.*, vol. 121, no. 6, p. 064802, Aug. 2018. doi:10.1103/PhysRevLett.121.064802

[19] P. Emma *et al.*, "Experimental demonstration of energy-chirp control in relativistic electron bunches using a corrugated pipe", *Phys. Rev. Lett.*, vol. 112, no. 3, p. 034801, Jan. 2014. doi:10.1103/PhysRevLett.112.034801